Published in final edited form as:
Am J Sports Med. 2012 December ; 40(12): 2853–2861. doi:10.1177/0363546512462009.

Infrared Fiber Optic Probe Evaluation of Degenerative Cartilage Correlates to Histological Grading

Arash Hanifi[1], **Xiaohong Bi**[2], **Xu Yang**[2], **Beril Kavukcuoglu**[1], **Ping Chang Lin**[3], **Edward DiCarlo**[2], **Richard G. Spencer**[3], **Mathias P.G. Bostrom**[2], and **Nancy Pleshko**[1,*]

[1]Department of Bioengineering, Temple University, Philadelphia, PA 19122

[2]Research Division, Hospital for Special Surgery, New York, NY10021

[3]The National Institute on Aging, National Institutes of Health, Baltimore, MD 21224

Abstract

Background—Osteoarthritis (OA), a degenerative cartilage disease, results in alterations of the chemical and structural properties of the tissue. Arthroscopic evaluation of full-depth tissue composition is limited and would require tissue harvesting, which is inappropriate in daily routine. Fourier transform infrared (FT-IR) spectroscopy is a modality based on molecular vibrations of matrix components that can be used in conjunction with a fiber optic to acquire quantitative compositional data from the cartilage matrix.

Purpose—To develop a model based on infrared spectra of articular cartilage to predict the histological Mankin score as an indicator of tissue quality.

Study Design—Descriptive laboratory study

Methods—Infrared fiber optic probe (IFOP) spectra were collected from nearly normal and more degraded regions of tibial plateau articular cartilage harvested during knee arthroplasty (N = 61). Each region was graded using a modified Mankin score (MMS). A multivariate partial least squares (PLS) algorithm using second derivative spectra was developed to predict histological MMS.

Results—The PLS model derived from IFOP spectra predicted the MMS with a prediction error of ~1.4, which resulted in ~72% of the Mankin scored tissues being predicted correctly, and 96% being predicted within one grade of their true modified Mankin score.

Conclusion—These data demonstrate that IFOP spectral parameters correlate with histological tissue grade, and can be used to provide information on tissue composition.

Clinical Relevance—IFOP studies have significant potential for evaluation of cartilage tissue quality without the need for tissue harvest. Combined with arthroscopy, IFOP analysis could facilitate definition of tissue margins in debridement procedures.

[*]Corresponding Author: Nancy Pleshko, Department of Bioengineering, Temple University, 1947 N. 12th St. Philadelphia, PA 19122, Tel: (215) 204-4280 npleshko@temple.edu.

Keywords

Cartilage; Osteoarthritis; Fourier Transform Infrared Spectroscopy; Histological Score; Arthroscopy

INTRODUCTION

Articular cartilage provides frictionless movement between joints while with standing repetitive mechanical stress. Cartilage has very limited capacity for self-repair, so the end-stage of degeneration, as a result of injury or osteoarthritis (OA), often leads to total knee arthroplasty (TKA). OA of the knee is also one of the most common causes of mobility restriction in the United States[23] and the number of primary TKA procedures is projected to grow to 3.48 million by 2030.[31] Initial treatment of degenerated cartilage consists of symptomatic pain relief through the use of anti-inflammatory agents.[53] For most of the cases arthroscopic procedures are performed to minimize the impact of articular cartilage irregularities. Success of these procedures, which include smoothing of roughened cartilage surfaces (shaving) and joint lavage and debridement, has been variable.[22] Biological cartilage repair procedures that aim to stimulate tissue repair of a focal defect, such as microfracture and autologous cartilage implantation (ACI) are also of great interest. However, the composition and structure of the repair tissue formed has also been variable, and typically includes fibrocartilage.[27, 47]

At the microscopic level, histologic features of osteoarthritic cartilage include a damaged collagen network, loss of cartilage zonal properties, decrease in proteoglycan (PG), and proliferation of chondrocytes.[53] Detection of such matrix changes in the early stages of OA, when treatment may prevent further cartilage damage, is critical for OA management. For arthroscopic repair, knowledge of specific ultrastructural changes would be extremely beneficial in making decisions regarding salvaging or removing cartilage and meniscus.

Several imaging techniques, including magnetic resonance imaging (MRI), ultrasound, and computed tomographic arthrography, have been explored to characterize early signs of OA, with non-invasive MRI being the most widely used.[12, 14, 25, 42, 54] Historically MRI has been used as a method for anatomic analysis, with the effect of disease progression on cartilage being evaluated with respect to such parameters as cartilage volume, thickness and surface characteristics.[12, 43] More recently, MRI has been used to study not only anatomy, but also biophysical properties of cartilage.[9, 44] While it is clear that MRI has the potential for early detection of molecular changes based on such properties, MRI clinically applicable methods for widespread use have not yet been established.

Fourier transform infrared (FT-IR) spectroscopy has been used extensively in recent years to characterize the structure and composition of normal, diseased and repair cartilage, as well as connective tissues such as tendon and bone.[10, 26] This technique provides information about the molecular structure of biomolecules, and is sensitive to compositional alterations in the tissue that accompany disease and repair. Many studies use FT-IR imaging spectroscopy (FT-IRIS), a technique which couples an FT-IR spectrometer to an array detector and an optical microscope, thus allowing mapping of specific molecules in the

tissue at high pixel resolution within a defined region of interest.[4, 6, 7, 10, 11, 13, 26, 29, 30, 45, 46] An additional advantage of FT-IR is the coupling of an infrared fiber optic probe (IFOP) to an FTIR spectrometer. This device provides spectral acquisition from intact tissues in situ, with the potential for in vivo assessments. Our laboratory has previously reported the application of an IFOP to evaluate degenerative cartilage in harvested human tissues, in addition to identification of specific spectral parameters that are related to early collagen degradation.[32, 56] A partial least squares (PLS) analysis method was used to correlate spectral data acquired from an IFOP to the Collins visual score for degenerative cartilage. Further studies were performed to monitor disease progression in an OA rabbit model,[7] where a PLS model based on IFOP data obtained from femoral cartilage yielded a correlation to disease course with an accuracy of over 90%. Together, these studies support the potential use of an IFOP for clinical diagnosis and therapeutic evaluation.

Ideally, IFOP investigations of cartilage would yield information on compositional changes in the tissue at the time of arthroscopy, and would therefore aid in disease management. Accordingly, the present study investigated changes in the structure and composition of articular cartilage from human knee joints with early and progressively severe degrees of OA using an IFOP, and compared data to histological grading and FT-IRIS data. The primary goal was to establish correlations between IFOP analysis of cartilage and a gold standard method of assessment of OA progression, histological evaluation according to Mankin.[34, 35]

MATERIALS AND METHODS

Human Tissue Collection

Under an IRB-approved protocol (Hospital for Special Surgery, #28006), human tibial plateaus were acquired from 61 male and female patients, 46-87 years of age, undergoing knee replacement surgery. The tibial plateaus were immediately brought to the laboratory in saline solution to maintain hydration once harvested, visually examined and regions of interest identified and graded using the Collins visual grading system based on the severity of cartilage softening and erosion.[16] Grades 0, 1, 2, and 3 represent a normal surface, slight superficial swelling or fibrillation, deeper fibrillation or serious fibrillation, respectively. Digital photographs were obtained from each specimen to record the position of spectral acquisition (Figure 1).

IFOP Data Acquisition

The design of the IFOP system has been described previously.[32] A Bruker infrared spectrometer (Billerica, MA) equipped with a mercury cadmium telluride (MCT) detector was coupled to a fiber optic probe, the end of which is a flat-tipped ZnS attenuated total reflectance (ATR) crystal of 1 mm diameter (Figure 1). The tip of the probe was placed in direct contact with individual regions on the tibial plateau specimen. Contact between the ATR crystal and the tibial plateau cartilage was monitored by a load cell with pressure controlled at 0.7 lb. Infrared data collection was initiated after a period of ~ 60 seconds of contact between the cartilage and crystal to permit relaxation of the cartilage around the

crystal tip.[56] Spectral acquisition from 4000–900 cm^{-1} with a spectral resolution of 8 cm^{-1} took approximately 1 minute for 256 co-added scans. Two to three regions from each tibial plateau were selected for sampling and 1-3 spectra/region were collected. Tissues were kept moist with saline solution, and additional saline added between data acquisitions if necessary. A total of 152 infrared spectra were used in the analyses, which corresponds to the number of spectra associated with tissues that were histologically graded by two independent observers.

Tissue Processing

Immediately following IFOP data acquisition, full-depth cartilage explants were harvested with a 5 mm diameter biopsy punch from the regions of the tibial plateau from which IFOP data were acquired. Explants were embedded in paraffin following tissue dehydration with 80% ethanol, PG containment using 1% cetylpyridiniumcholoride, and decalcification with 10% EDTA/Tris buffer. Histological sections were cut perpendicular to the articular surface with thickness of 7 microns (for FT-IRIS) and 6 microns (for histology) and mounted onto BaF_2 infrared windows and glass slides for FT-IRIS and histological analysis, respectively. All sections were deparaffinized prior to FT-IRIS measurements.

Histological Evaluation

Histological sections were stained with safranin O and with hematoxylin and eosin (H&E) for evaluation of PG content, and tissue and cellular morphology. The stained tissue slides were evaluated by two investigators in a random and blind-coded manner according to a modified Mankin grading system. The histological Mankin score is a standard grading system for cartilage based on structural fissuring, cell cloning, loss of PG, and tidemark integrity.[34, 35] The modified Mankin scoring (MMS) system used in the current study ranged from Grade 0, which represents normal cartilage, to Grade 13, which represents severely degraded cartilage (Table 1). A final MMS was calculated as a mean of the two evaluations. and therefore, half integer values were possible. Interobserver agreement was calculated using the Fleiss weighted Kappa statistic.[24] Correlations between individual components of the MMS and the total MMS were investigated using a Pearson correlation with significance determined at the $p<0.05$ level.

Partial Least Squares (PLS) Analysis

IFOP spectra (n = 152) obtained from tissues with modified Mankin scores that ranged from 2 – 10 (this was the full range of MMSs found in tissues used in the current study) were analyzed using a partial least squares (PLS) regression algorithm.[7, 58] Prior to PLS analysis, spectra were processed by a multiplicative scatter correction (MSC) and 13-point Savitzky–Golay second derivative calculation. As absorbances from molecules in varying tissue environments can contribute to the broad contours of infrared spectral bands, applying a second derivative calculation to the spectra essentially improves the spectral resolution.[36] Several frequency regions were investigated for analysis, and ultimately, the preprocessed values for frequencies in the region of 1800– 984 cm^{-1} were used as variables to predict the average MMS of two investigators. This frequency range includes absorbances from all primary matrix components of cartilage.

A leave-one-out cross validation was used to create three separate PLS models. Each of the three models included data from 100 randomly chosen spectra, with the remaining 52 spectra serving as an independent prediction set. PLS decomposes information carried by the original variables (spectra) and projects them onto a smaller number of latent variables called “factors”. In infrared spectroscopy, the factors resemble spectra, but don’t necessarily reflect the spectrum of an individual tissue component. In creating the PLS model, there is an optimal number of factors that together can explain the variance in all regions of the spectrum. The number of factors for all models was calculated to be seven, based on the minimal residual sum of squares error (SS_{err}).[20] Based on a leverage versus residual scatter plot of the PLS model[20], no outliers were detected in the PLS cross-validation models. The quality of the models was evaluated by assessment of the root mean square error (RMSE) of the cross validation model. RMSE measures the precision of the model and is calculated according to the equation below:

$$RMSE = \sqrt{\frac{\sum (Y\,prediction(i) - Y\,experiment(i))^2}{N}} \quad \text{Equation 1}$$

(i: number of samples = 1 to N).[2, 15]

The quality of the independent prediction of each sample MMS was assessed by evaluation of the root mean square error of prediction (RMSEP). The averaged results from the three PLS models are presented in Table 2. The Unscrambler software (CAMO Software, Oslo, Norway) was used for all calculations.

FT-IRIS Data Acquisition and Processing

Due to the complexity of the FT-IRIS data analysis, FT-IRIS data were collected from just a subset of histological tissue sections to assess full-depth tissue molecular changes across a range of modified Mankin scores (N = 28). Tissues had previously been sampled by IFOP and Mankin-graded. Sections were sampled at 8 cm^{-1} spectral resolution and 6.25-μm pixel resolution using a Spectrum Spotlight 300 FT-IR Imaging system (Perkin-Elmer, Bucks, UK), which couples a FTIR spectrometer with an array detector and a light microscope. Polarized FT-IRIS measurements were performed with apolarizer inserted in the incident light path at 0°. Figure 2 illusturates typical infrared spectra of cartilage of different histological grades where the bands associated with the vibrations of collagen and proteoglycan are labeled. In general, molecular information can be obtained from IR images based on the area under an absorbance peak, or peak height ratios, that are related to specific molecular components.[10] ISys software v4.0 (Malvern, UK) was used for all FT-IRIS data processing. Assessment of collagen was based on the integrated area of the protein amide I absorbance band (1598 – 1710 cm^{-1}) and assessment of PG based on the integrated area of the absorbance between 950 – 1150 cm^{-1} that arises from the sugar ring vibrations in proteoglycans.

The area ratio of the IR absorbance centered at 1338 cm^{-1} (1300 – 1356 cm^{-1}), which arises from collagen side chain vibrations, to the amide II absorbance (1492 – 1598 cm^{-1}) was calculated to evaluate the helical integrity of collagen, a parameter previously shown to correlate to collagen degradation in cartilage.[57] The peak height ratio in the amide I band at

1660/1690 cm^{-1} was used as an indicator of collagen maturity, as shown in previous studies.[10, 21] Collagen fibril orientation was calculated as the ratio of the area ratio of amide I and amide II bands of the polarized IR images. The collagen fibril orientation was quantitated as fibrils parallel to the articular surface for an amide I/II polarized ratio ≥2.7; fibrils perpendicular to the articular surface for an amide I/II ratio ≤1.7, and random or mixed fibril orientation for amide I/II ratios between 2.7–1.7.[6]

Statistical Analysis

FT-IRIS parameters were calculated for Mankin-graded samples at each pixel. All data are presented as mean ± standard deviation. Statistical comparisons among the grades were performed by oneway ANOVA followed by Bonferroni correction post-hoc tests for comparison of groups with values significant at the $p<0.05$ level. A Pearson correlation was performed to assess the relationship between individual components of the Mankin score and the total Mankin score.

RESULTS

Histology Grading

Modified Mankin scores of the tissues ranged from 2 to 10, and the weighted interobserver agreement between graders was 86%, which is categorized as excellent agreement.[24] In general, tissue thickness decreases and fibrillation increases with increasing degradation (Figure 3A, B). Correlation between MMS and Collins visual grade did not reach significance ($R = 0.29$, $p = 0.09$), indicating that the visual grade of the tissues may not reflect microstructure and composition. The greatest correlation between an individual component of the MMS and the total MMS was with structural fissuring ($R = 0.64$), followed by tidemark integrity ($R = 0.60$), cell cloning ($R = 0.50$), and PG content ($R = 0.40$). All individual components were significantly correlated to total MMS ($p < 0.01$).

PLS Analysis of IFOP Spectra

Qualitatively, progressive changes are seen in several regions of IFOP spectra from tissues with increasing degradation (Figure 2), including differences in the contours and relative intensity ratios of the amide I and amide II absorbances. It is known that there is a strong infrared water absorbance that overlaps the protein amide I region,[56] and this likely contributes to the observed spectral changes. In addition, fewer distinct spectral features are observed across many frequencies in the more degraded tissues with higher MMSs. Together, these observations support the use of a multivariate analysis to evaluate spectral changes.

The PLS models were able to predict the Mankin score with an average prediction error of 1.41. The average percentage of correctly predicted tissue grades for the three models was 72 (±3.1)%, and the average percentage of tissue grades that were predicted within one of their actual grade was 96 (±1.4)% (Table 2).

FT-IRIS Analysis

FT-IRIS analysis was performed on a subset of tissues to assess full-depth tissue compositional changes. In general, average collagen content was variable, but greater in some of the more degraded tissues with a higher Mankin score, a phenomenon likely attributable to decreased relative amount of superficial and mid zones in these tissues. PG content was also very variable (Table 3). However, no significant differences in collagen or PG were found at any time point. Collagen integrity also did not differ among the tissues. However, collagen maturity significantly decreased with increasing MMS ($p = 0.032$), (Figure 4). In addition, collagen fibril orientation changes were evident with tissue degradation (Table 3, Figure 5). Parallel fibril orientation decreased significantly ($p=0.024$), while random and perpendicular fibril orientation increased significantly ($p=0.005$) as MMS increased. Thinning of the superficial zone likely contributed to this phenomenon.

DISCUSSION

The results of the present study demonstrate the ability of infrared spectroscopy together with a PLS multivariate analysis to predict the histologic Mankin score of degenerative articular cartilage. The PLS model was able to predict 72% of the Mankin score values correctly, and 96% within one grade of their true MMS. As IFOP data is only collected from the top ~ 10 μm of the tissue surface, and Mankin grading includes evaluation of the entire tissue depth, it is evident that tissue surface changes detectable by IFOP reflect full-depth changes. In view of this, it was not surprising that the greatest correlation of the total MMS with an individual component of the score was with surface structural changes. A strong correlation between total Mankin score and surface structural changes was also demonstrated in previous studies.[48]

Arthroscopic assessment of articular cartilage is based primarily on visual evaluation, and serves as a decision-making process for treatment options.[28] Interestingly, in the current study, the correlation between visual assessment of cartilage and histologic Mankin score did not reach significance. This leads to the question of whether visual inspection of cartilage is sufficient to assess the quality of the tissue. The goal of many arthroscopic procedures is to remove damaged areas of tissues,[38] and controversy still surrounds the effectiveness of these procedures.[5] There can be a high interobserver variability in arthroscopic grading of cartilage, and the final grade can be highly subjective, and dependent on the level of clinical experience of the surgeon.[37] It is possible that tissue regions that appear visually normal may indeed have begun to degenerate, and thus should be removed. Attempts to identify such regions, although not possible visually, may be possible using either indentation or spectroscopic methods, or a combination of these two. Duda et al[19] and Bae et al.[3] used an indentation probe to assess whether tissue stiffness reflects cartilage degeneration. In both studies, it was demonstrated that indentation stiffness decreases as cartilage degeneration progresses to mild stages. However, the clinical application of the instrument was limited buy its large dimensions. In addition, the probe needed to be positioned exactly vertical to the cartilage surface which also limits the potential applications.[51] Accordingly, development of infrared spectroscopy techniques as a

minimally invasive arthroscopic method that can provide information on the quality of the full tissue depth in vivo is certainly a point of interest.

In the current study, the gold standard for comparison to infrared spectra was a modified Mankin score. The reliability and reproducibility of osteoarthritic cartilage histopathology grading systems, including Mankin and the Osteoarthritis Research Society International (OARSI) cartilage histopathology assessment system, have been evaluated in several studies.[18, 39, 41, 55] In one study, a comparison of Mankin grading by two observers found inadequate reproducibility (59-76%), and the ability to detect differences between normal and moderate OA was also uncertain. In addition, the wide range of chemical and structural changes in OA cartilage contributed to limited reliability of the scoring systems and high interobserver variability.[55] Ostergaard et al. examined the interobserver and intraobserver reproducibility of the Mankin grading system of human articular cartilage using Kappa analysis. They found that there was a low intraobserver agreement (22%-33%) of the Mankin score, based on repeated grading of the same sample by the same observer at different times, and a wide variation of interobserver reproducibility (13%-20%), possibly because of the lack of experience of observers. It was concluded that the semi-quantitative values obtained from the Mankin system are a result of subjective evaluation and are not adequately reproducible for assessment of OA cartilage.[39, 40] Nevertheless, histologic grading of OA cartilage remains the gold standard for comparison to other modes of evaluation,[41] and there have been significant research efforts to improve its reliability, reproducibility and validity.[18] In the current study, the interobserver agreement was 86%, which is higher than reported in several other studies. This may be due to the two graders having been trained to grade tissues at the same time by an experienced pathologist. In general, compared to histological grading, spectroscopic assessment has inherently less subjectivity associated with the measurement, and may therefore be more accurate.

The sensitivity of infrared spectral changes to cartilage degradation was established in previous studies from our group, where IFOP analysis was used to assess OA cartilage in early stages of degeneration.[56] Specific spectral changes related to early stages of the disease were identified, including changes in the collagen amide II, amide III and the 1338 cm^{-1} regions of the IFOP spectra. These changes were also identical in FT-IRIS data, where degenerated tissues showed a significantly higher amide II/1338 cm^{-1} area ratio.[56] A follow-up study investigated whether multivariate analysis of IFOP spectra could be used to predict Collins visual grade of degraded tibial plateaus.[32] Although a correlation was found between the infrared spectra and Collins visual grade, 15 factors were required to obtain a reasonable model of prediction, indicative of the large amount of variability that contributes to that model. Combined with the knowledge that the Collins visual grade and histological Mankin score do not significantly correlate, it's preferable to use the current PLS model to assess cartilage structural changes.

In situ near infrared (NIR) spectroscopy with a fiber optic probe has also been used to assess the quality of articular cartilage[50]. The frequency range and penetration depth for NIR radiation are greater than for mid-infrared radiation, but the interpretation of NIR spectra remains challenging due to overlapping peaks from many components, and a much lower signal to noise ratio.[49] In a study by Spahn et al[50], there was only weak agreement among

the observers for visual evaluation of femoral and tibial cartilage degeneration, but a significant correlation among the NIR values measured by different surgeons. A challenge to this method was positioning the NIR probe accurately so that it was perpendicular to the articular surface, as it would be as well for the IFOP when used in vivo. Nevertheless, it was concluded that there is potential for development of a NIR spectroscopic probe for objective measurement of cartilage.

FT-IRIS data obtained from full depth tissues were investigated to better understand the compositional differences that contribute to the IFOP spectral changes. Although reduced PG content in OA cartilage has been reported previously,[7, 56] no significant changes in the mean PG content of the tissue was detected in FT-IRIS derived images in this study. In addition, changes in collagen also did not correspond with tissue degradation. It is known that in the cartilage degradation process, superficial and middle zone regions are lost, and thus it is difficult to directly compare the tissue in later stages of OA with tissue that is nearly intact. However, the FT-IRIS derived collagen maturity parameter (1660/1690 cm^{-1}) was found to decrease significantly during OA progression, reflective of an effect of disease progression on collagen fibril structure. The precise collagen modification that underlies this change is unknown.[21], but it is not surprising that disruption of the collagen network would result in a change in the primary infrared absorbance of collagen. Unfortunately, this parameter cannot easily be investigated in IFOP spectra, due to the presence of the water absorbance in this spectral region.

Degeneration of cartilage also results in changes in collagen fiber orientation.[1, 8, 17] Specifically, as the superficial regions of cartilage, which normally contain collagen fibers oriented parallel to the surface, are lost, the fraction of the collagen fibers parallel to the surface decreases significantly. A similar result was found in the current study, where a greater percentage of randomly oriented fibrils, and fibrils oriented perpendicular to the surface, were found in the more degraded tissues. Together, the FT-IRIS data show that, in addition to the compositional changes described in the modified Mankin grading, changes in collagen structure are progressive with degradation.

There are also limitations regarding use of the IFOP for cartilage assessment. The ATR probe crystal has a 1 mm diameter, which therefore represents the smallest tissue diameter that can be evaluated. Although much larger than the micron diameters that are possible with imaging data acquisition, this could be sufficient in clinical determination of the margins of a tissue lesion that requires excision or debridement. Another current limitation is the outer diameter of the fiber optic cable, ~ 7mm. For arthroscopic interrogation of the tissue, an individual entry port for the IFOP would be required that may be slightly larger than that required for the optical arthroscopic fiber, which is on the order of 3-5mm.[52] In addition, the current prototype IFOP requires tissue contact at a 90 degree angle, similar to the requirements for the mechanical indentation probe,[3, 19] which limits access and therefore not all cartilage regions can be evaluated. However, these geometric issues can be overcome, as narrower diameter infrared fiber optics are under development,[33] as well as “side-facing” probes. For the laboratory study, a load cell was used to record the force of the probe tip on the cartilage sample and maintain it at a constant level for data reproducibility. In vivo, a feedback mechanism would have to be incorporated into the handle of the probe to maintain

a constant force. Lastly, another potential limitation during in vivo assessment of cartilage is interference from absorbances present in synovial fluid and blood. These may overlap with absorbances from the proteins in cartilage, and have to be taken into account during data processing. The laboratory studies performed here did not address these potential complexities in data analysis, but infrared studies of cartilage assessment in the in vivo environment are underway, and will focus on these issues.

In summary, this study presents development of a spectroscopic method combined with multivariate analysis to predict the quality of the cartilage tissue in early-to-late stages of OA. The results indicate that in the clinical environment, spectral acquisition and processing to predict the Mankin score of a region on the surface of articular cartilage could be performed within a short period of time. There would not be any further implications for surgeons other than placing the probe in contact with the area of interest. Thus, a relatively fast, in vivo, fiber optic technique could be used to provide spectral information that will be analyzed in real-time using an optimized PLS model with a user-friendly software interface, yielding compositional information that may be substantially more accurate than visual assessment of the tissue.

Acknowledgments

This study was supported by NIH EB00744 (NP) and the National Institute on Aging, NIH, intramural program (RGS), and utilized an NIH-supported Musculoskeletal Core Facility (AR46121).

Experimental work for this study was performed at Hospital for Special Surgery, and data analyses performed at Hospital for Special Surgery, Temple University and The National Institute on Aging.

References

1. Alhadlaq HA, Xia Y, Moody JB, Matyas JR. Detecting structural changes in early experimental osteoarthritis of tibial cartilage by microscopic magnetic resonance imaging and polarised light microscopy. Annals of the Rheumatic Diseases. Jun; 2004 63(6):709–717. [PubMed: 15140779]
2. Aptula AO, Jeliazkova NG, Schultz TW, Cronin MTD. The better predictive model: High q(2) for the training set or low root mean square error of prediction for the test set? Qsar & Combinatorial Science. Apr; 2005 24(3):385–396.
3. Bae WC, Temple MM, Amiel D, Coutts RD, Niederauer GG, Sah RL. Indentation testing of human cartilage: sensitivity to articular surface degeneration. Arthritis Rheum. Dec; 2003 48(12):3382–3394. [PubMed: 14673990]
4. Baykal D, Irrechukwu O, Lin PC, Fritton K, Spencer RG, Pleshko N. Nondestructive assessment of engineered cartilage constructs using near-infrared spectroscopy. Appl Spectrosc. Oct; 2010 64(10): 1160–1166. [PubMed: 20925987]
5. Bernstein J, Quach T. A perspective on the study of Moseley et al: questioning the value of arthroscopic knee surgery for osteoarthritis. Cleve Clin J Med. May; 2003 70(5):401, 405–406, 408–410. [PubMed: 12779130]
6. Bi X, Li G, Doty SB, Camacho NP. A novel method for determination of collagen orientation in cartilage by Fourier transform infrared imaging spectroscopy (FT-IRIS). Osteoarthritis Cartilage. 2005; 13(12):1050–1058. [PubMed: 16154778]
7. Bi X, Yang X, Bostrom M, et al. Fourier transform infrared imaging and MR microscopy studies detect compositional and structural changes in cartilage in a rabbit model of osteoarthritis. Analytical and Bioanalytical Chemistry. 2007; 387(5):1601–1612. [PubMed: 17143596]
8. Bi X, Yang X, Bostrom MPG, Camacho NP. Fourier transform infrared imaging spectroscopy investigations in the pathogenesis and repair of cartilage. Biochimica et Biophysica Acta (BBA) - Biomembranes. 2006; 1758(7):934–941.

9. Black BR, Chong le R, Potter HG. Cartilage imaging in sports medicine. Sports Med Arthrosc. Mar; 2009 17(1):68–80. [PubMed: 19204554]
10. Boskey A, Pleshko Camacho N. FT-IR imaging of native and tissue-engineered bone and cartilage. Biomaterials. 2007; 28(15):2465–2478. [PubMed: 17175021]
11. Brama PA, Holopainen J, van Weeren PR, Firth EC, Helminen HJ, Hyttinen MM. Influence of exercise and joint topography on depth-related spatial distribution of proteoglycan and collagen content in immature equine articular cartilage. Equine Vet J. Jul; 2009 41(6):557–563. [PubMed: 19803051]
12. Burgkart R, Glaser C, Hyhlik-Durr A, Englmeier KH, Reiser M, Eckstein F. Magnetic resonance imaging-based assessment of cartilage loss in severe osteoarthritis: accuracy, precision, and diagnostic value. Arthritis Rheum. Sep; 2001 44(9):2072–2077. [PubMed: 11592369]
13. Camacho NP, West P, Torzilli PA, Mendelsohn R. FTIR microscopic imaging of collagen and proteoglycan in bovine cartilage. Biopolymers. 2001; 62(1):1–8. [PubMed: 11135186]
14. Chung CB, Frank LR, Resnick D. Cartilage imaging techniques: current clinical applications and state of the art imaging. Clin Orthop Relat Res. Oct.2001 (391 Suppl):S370–378. [PubMed: 11603720]
15. Coleman MD, Gardiner TD. Sensitivity of model-based quantitative FTIR to instrumental and spectroscopic database error sources. Vibrational Spectroscopy. Nov 10; 2009 51(2):177–183.
16. Collins, DH. The Pathology of Articular and Spinal Diseases. London: 1949.
17. Curtin WA, Reville WJ. Ultrastructural Observations on Fibril Profiles in Normal and Degenerative Human Articular-Cartilage. Clinical Orthopaedics and Related Research. Apr.1995 (313):224–230. [PubMed: 7641485]
18. Custers RJ, Creemers LB, Verbout AJ, van Rijen MH, Dhert WJ, Saris DB. Reliability, reproducibility and variability of the traditional Histologic/Histochemical Grading System vs the new OARSI Osteoarthritis Cartilage Histopathology Assessment System. Osteoarthritis Cartilage. Nov; 2007 15(11):1241–1248. [PubMed: 17576080]
19. Duda GN, Kleemann RU, Bluecher U, Weiler A. A new device to detect early cartilage degeneration. Am J Sports Med. Apr-May;2004 32(3):693–698. [PubMed: 15090387]
20. Esbensen, KH. Multivariate data analysis-in practice. 5. Oslo, Norway: Camo; 2002.
21. Farlay D, Duclos ME, Gineyts E, et al. The Ratio 1660/1690 cm(-1) Measured by Infrared Microspectroscopy Is Not Specific of Enzymatic Collagen Cross-Links in Bone Tissue. Plos One. Dec 14.2011 6(12)
22. Felson DT. Arthroscopy as a treatment for knee osteoarthritis. Best Pract Res Clin Rheumatol. Feb; 2010 24(1):47–50. [PubMed: 20129199]
23. Felson DT. Osteoarthritis in 2010: New takes on treatment and prevention. Nat Rev Rheumatol. Feb; 2011 7(2):75–76. [PubMed: 21289610]
24. Fleiss JL. Measuring Nominal Scale Agreement among Many Raters. Psychological Bulletin. 1971; 76(5):378.
25. Grunder W. MRI assessment of cartilage ultrastructure. NMR Biomed. Nov; 2006 19(7):855–876. [PubMed: 17075962]
26. Hanifi A, Richardson J, Kuiper J, Roberts S, Pleshko N. Clinical Outcome of Autologous Chondrocyte Implantation Is Correlated With Infrared Spectroscopic Imaging-Derived Parameters. Osteoarthritis and Cartilage. 2012 In Press.
27. Hunziker EB. Articular cartilage repair: basic science and clinical progress. A review of the current status and prospects. Osteoarthritis and Cartilage. 2002; 10(6):432–463. [PubMed: 12056848]
28. Jackson RW, DeHaven KE. Arthroscopy of the knee. Clin Orthop Relat Res. 1975; (107):87–92. [PubMed: 1173357]
29. Kim M, Foo LF, Uggen C, et al. Evaluation of Early Osteochondral Defect Repair in a Rabbit Model Utilizing Fourier Transform-Infrared Imaging Spectroscopy, Magnetic Resonance Imaging, and Quantitative T2 Mapping. Tissue Engineering Part C: Methods. 2010; 16(3):355–364. [PubMed: 19586313]
30. Kobrina Y, Rieppo L, Saarakkala S, Jurvelin J, Isaksson H. Clustering of infrared spectra reveals histological zones in intact articular cartilage. Osteoarthritis Cartilage. May; 2012 20(5):460–468. [PubMed: 22333731]

31. Kurtz S, Ong K, Lau E, Mowat F, Halpern M. Projections of primary and revision hip and knee arthroplasty in the United States from 2005 to 2030. J Bone Joint Surg Am. Apr; 2007 89(4):780–785. [PubMed: 17403800]
32. Li G, Thomson M, Dicarlo E, et al. A chemometric analysis for evaluation of early-stage cartilage degradation by infrared fiber-optic probe spectroscopy. Appl Spectrosc. Dec; 2005 59(12):1527–1533. [PubMed: 16390593]
33. Mackanos MA, Contag CH. Fiber-optic probes enable cancer detection with FTIR spectroscopy. Trends in Biotechnology. Jun; 2010 28(6):317–323. [PubMed: 20452071]
34. Mankin HJ, Dorfman H, Lippiello L, Zarins A. Biochemical and metabolic abnormalities in articular cartilage from osteo-arthritic human hips. II. Correlation of morphology with biochemical and metabolic data. J Bone Joint Surg Am JID - 0014030. 1971; 53(3):523–537.
35. Mankin HJ, Lippiello L. Biochemical and metabolic abnormalities in articular cartilage from osteo-arthritic human hips. J Bone Joint Surg Am JID - 0014030. 1970; 52(3):424–434.
36. Mark H, Workman J. Derivatives in spectroscopy Part I - The behavior of the derivative. Spectroscopy. Apr; 2003 18(4):32–37.
37. Marticke JK, Hosselbarth A, Hoffmeier KL, et al. How do visual, spectroscopic and biomechanical changes of cartilage correlate in osteoarthritic knee joints? Clin Biomech (Bristol, Avon). May; 2010 25(4):332–340.
38. Moseley JB, O'Malley K, Petersen NJ, et al. A controlled trial of arthroscopic surgery for osteoarthritis of the knee. N Engl J Med. Jul 11; 2002 347(2):81–88. [PubMed: 12110735]
39. Ostergaard K, Andersen CB, Petersen J, Bendtzen K, Salter DM. Validity of histopathological grading of articular cartilage from osteoarthritic knee joints. Ann Rheum Dis. Apr; 1999 58(4): 208–213. [PubMed: 10364898]
40. Ostergaard K, Petersen J, Andersen CB, Bendtzen K, Salter DM. Histologic/histochemical grading system for osteoarthritic articular cartilage: reproducibility and validity. Arthritis Rheum. Oct; 1997 40(10):1766–1771. [PubMed: 9336409]
41. Pearson RG, Kurien T, Shu KS, Scammell BE. Histopathology grading systems for characterisation of human knee osteoarthritis--reproducibility, variability, reliability, correlation, and validity. Osteoarthritis Cartilage. Mar; 2011 19(3):324–331. [PubMed: 21172446]
42. Peterfy C, Kothari M. Imaging osteoarthritis: magnetic resonance imaging versus x-ray. Curr Rheumatol Rep. Feb; 2006 8(1):16–21. [PubMed: 16515760]
43. Peterfy CG. Scratching the surface: articular cartilage disorders in the knee. Magn Reson Imaging Clin N Am. 2000; 8(2):409–430. [PubMed: 10819921]
44. Potter HG, Black BR, Chong le R. New techniques in articular cartilage imaging. Clin Sports Med. Jan; 2009 28(1):77–94. [PubMed: 19064167]
45. Ramakrishnan N, Xia Y, Bidthanapally A. Polarized IR microscopic imaging of articular cartilage. Phys Med Biol. Aug 7; 2007 52(15):4601–4614. [PubMed: 17634653]
46. Rieppo L, Saarakkala S, Narhi T, Helminen HJ, Jurvelin JS, Rieppo J. Application of second derivative spectroscopy for increasing molecular specificity of fourier transform infrared spectroscopic imaging of articular cartilage. Osteoarthritis Cartilage. May; 2012 20(5):451–459. [PubMed: 22321720]
47. Roberts S, Hollander AP, Caterson B, Menage J, Richardson JB. Matrix turnover in human cartilage repair tissue in autologous chondrocyte implantation. Arthritis and Rheumatism. Nov; 2001 44(11):2586–2598. [PubMed: 11710715]
48. Rutgers M, van Pelt MJ, Dhert WJ, Creemers LB, Saris DB. Evaluation of histological scoring systems for tissue-engineered, repaired and osteoarthritic cartilage. Osteoarthritis Cartilage. Jan; 2010 18(1):12–23. [PubMed: 19747584]
49. Salzer, R.; Siesler, HW. Infrared and Raman Spectroscopic Imaging. Weinheim: Wiley-VCH Verlag GmbH & Co. KGaA; 2009.
50. Spahn G, Klinger HM, Baums M, et al. Near-infrared spectroscopy for arthroscopic evaluation of cartilage lesions: results of a blinded, prospective, interobserver study. Am J Sports Med. Dec; 2010 38(12):2516–2521. [PubMed: 20847221]

51. Spahn G, Plettenberg H, Kahl E, Klinger HM, Muckley T, Hofmann GO. Near-infrared (NIR) spectroscopy. A new method for arthroscopic evaluation of low grade degenerated cartilage lesions. Results of a pilot study. BMC Musculoskelet Disord. 2007; 8:47. [PubMed: 17535439]
52. Tingstad EM, Spindler KP. Basic arthroscopic instruments. Operative Techniques in Sports Medicine. 2004; 12(3):200–203.
53. Umlauf D, Frank S, Pap T, Bertrand J. Cartilage biology, pathology, and repair. Cell Mol Life Sci. Dec; 67(24):4197–4211. [PubMed: 20734104]
54. Van Breuseghem I. Ultrastructural MR imaging techniques of the knee articular cartilage: problems for routine clinical application. Eur Radiol. Feb; 2004 14(2):184–192. [PubMed: 14600779]
55. van der Sluijs JA, Geesink RG, van der Linden AJ, Bulstra SK, Kuyer R, Drukker J. The reliability of the Mankin score for osteoarthritis. J Orthop Res. Jan; 1992 10(1):58–61. [PubMed: 1727936]
56. West PA, Bostrom MPG, Torzilli PA, Camacho NP. Fourier transform infrared spectral analysis of degenerative cartilage: An infrared fiber optic probe and imaging study. Applied Spectroscopy. Apr; 2004 58(4):376–381. [PubMed: 15104805]
57. West PA, Torzilli PA, Chen C, Lin P, Camacho NP. Fourier transform infrared imaging spectroscopy analysis of collagenase-induced cartilage degradation. J Biomed Opt. 2005; 10(1): 14015. [PubMed: 15847596]
58. Wold S, Sjostrom M, Eriksson L. PLS-regression: a basic tool of chemometrics. Chemometrics and Intelligent Laboratory Systems. Oct 28; 2001 58(2):109–130.

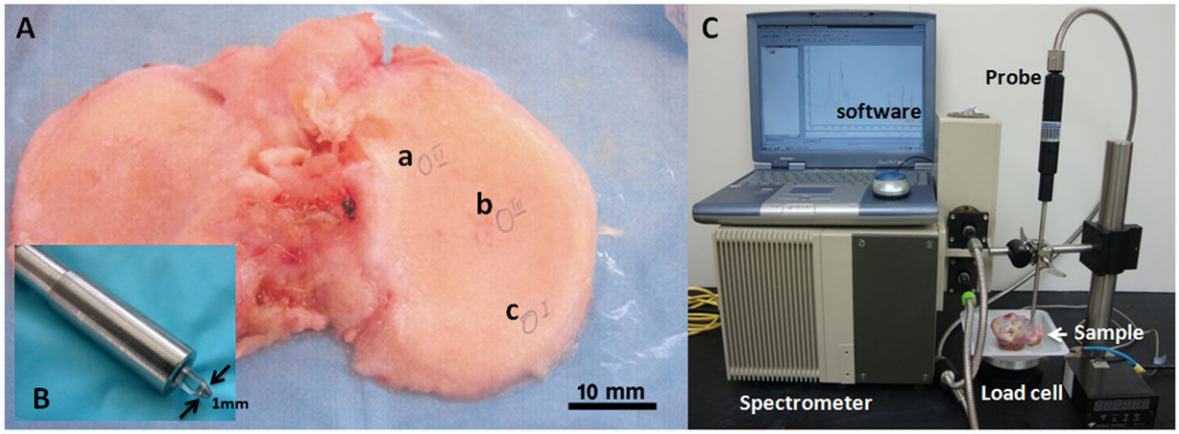

Figure 1.

A) A typical tibial plateau used for spectroscopic analysis with the positions of data acquisition marked as a (Collin score II, MMS 5.5), b (Collins score II) and c (Collins score I). B) The flat-tipped ATR probe of 1 mm diameter. C). Spectrometer and infrared fiber optic probe in contact with a tibial plateau sample, The load cell under the sample records the force from contact of the fiber optic probe with the sample.

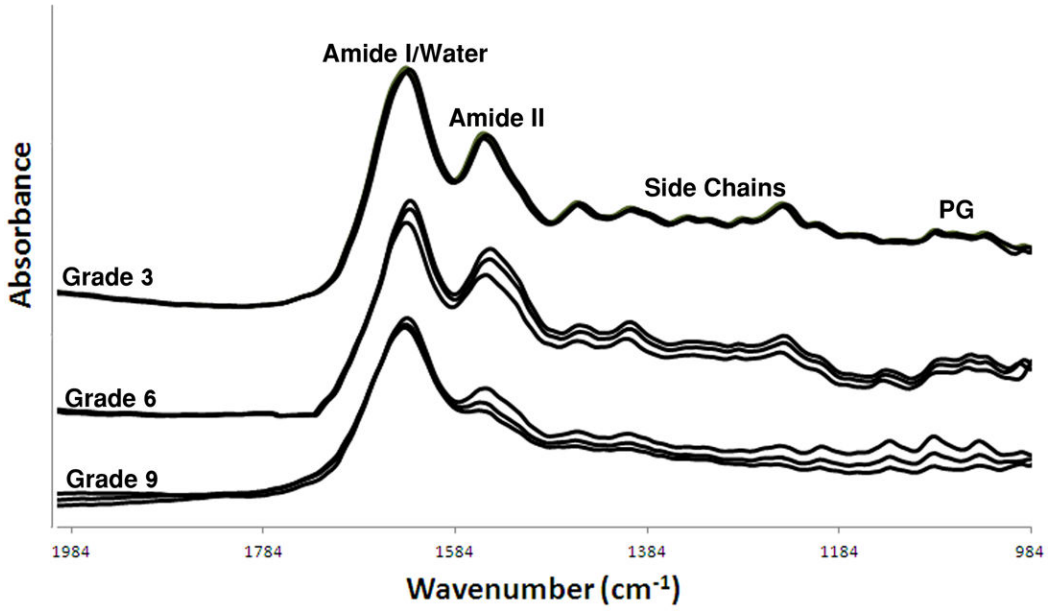

Figure 2.

IFOP spectra obtained from tibial plateau cartilage with modified Mankin scores of 3, 6 and 9, which are vertically offset for clarity. The absorbance bands associated with collagen amide and side chain vibrations, water, and proteoglycan sugar vibrations, are shown. Changes in spectral features, such as relative peak height and contour of the amide I/water and amide II absorbances, and reduced spectral features across the rest of the spectral frequencies, are evident with OA progression (increased Mankin score).

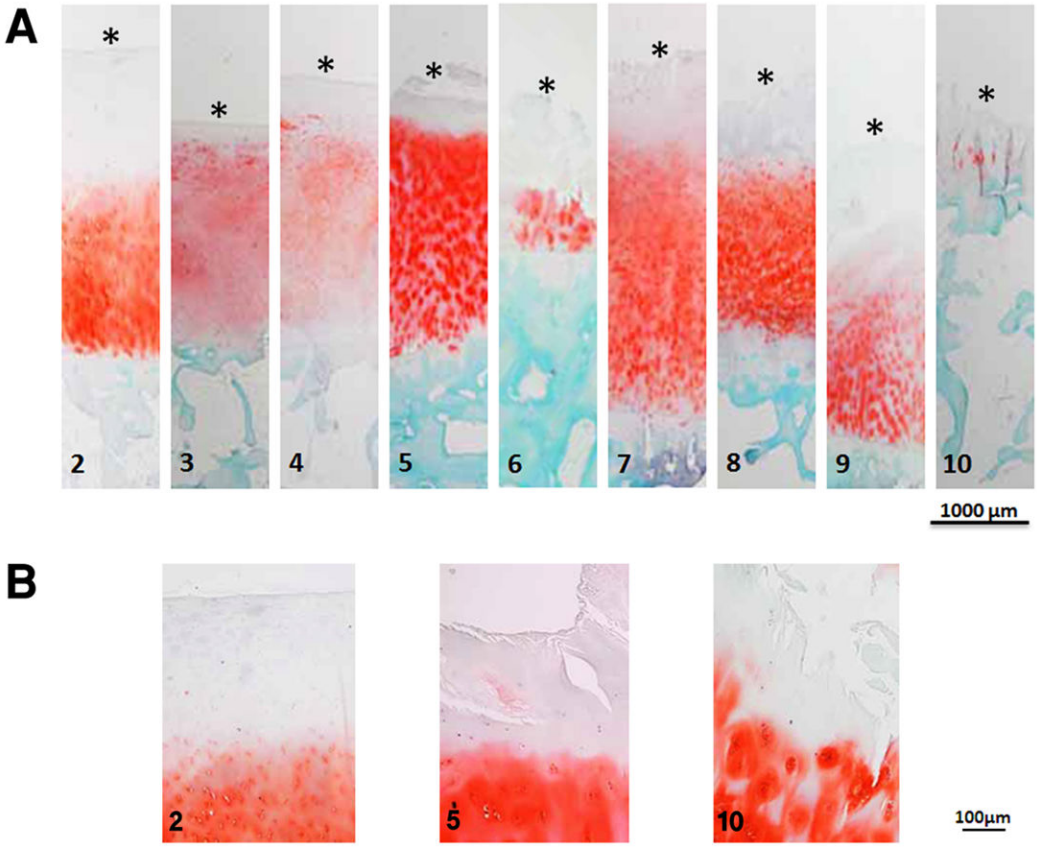

Figure 3.

A) Safranin O stained images of tibial plateau cartilage tissue sections with modified Mankin scores (MMS) of 2 to 10. In general, tissue thickness decreases with increasing MMS, and surface fibrillation increases. *****The surface of the tissue section is marked for clarity. B) Safranin O images of tissue with MMS 2, 5 and 10 with higher magnification that show increasing surface fibrillation with increasing MMS.

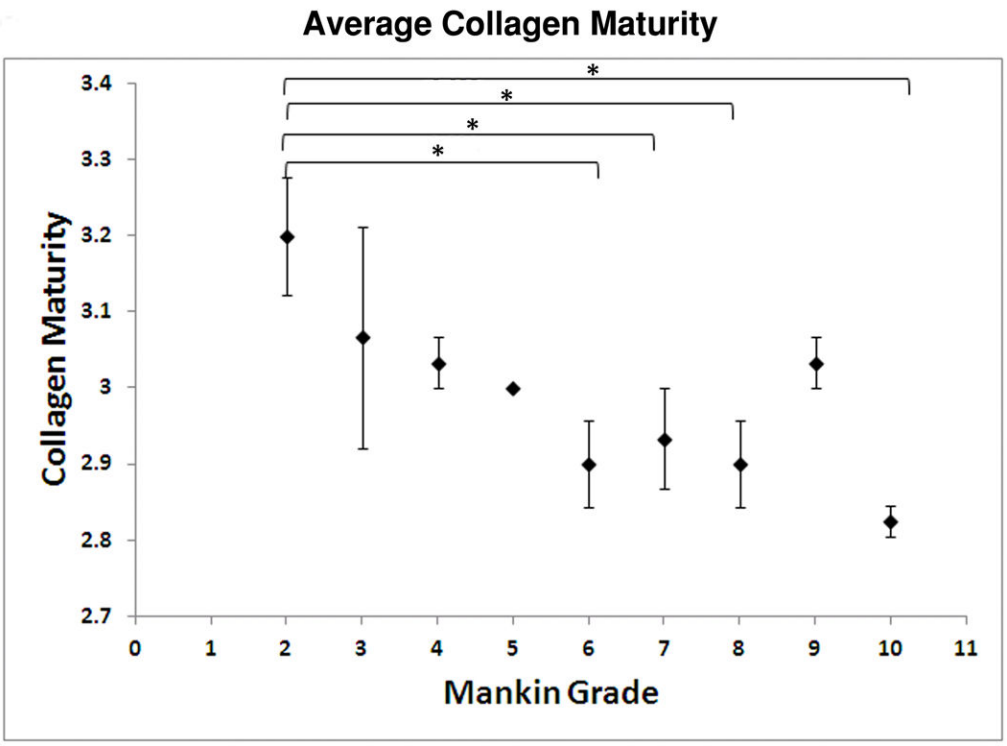

Figure 4.

FT-IRIS-derived values of collagen maturity averaged over the full depth of cartilage versus MMS. Data are plotted as mean ± standard error (* $p < 0.05$). In general, collagen maturity decreases as MMS increases.

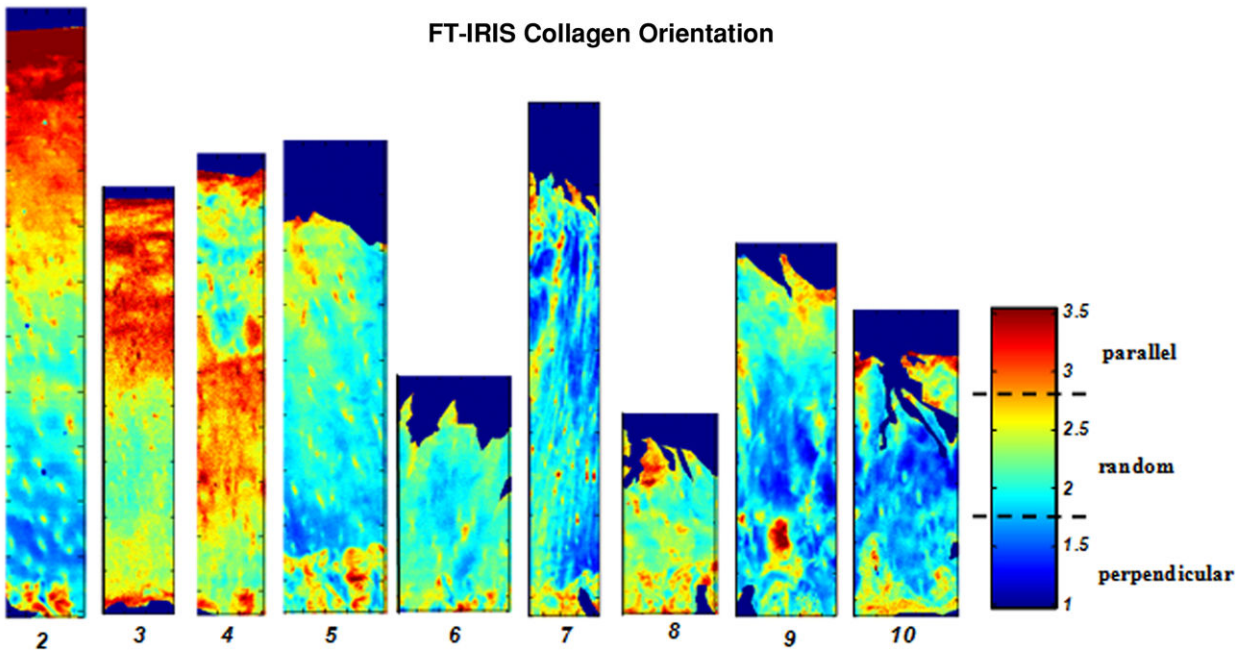

Figure 5.

FT-IRIS images based on the collagen fibril orientation of tibial plateau articular cartilage with modified Mankin scores 2-10. The color bar indicates the boundaries of parallel, perpendicular and randomly oriented fibrils. The percentage of the relative amount of parallel fibrils decrease, and random fibrils increase throughout the tissue as MMS increases.

Table 1

Modified Mankin Score[34, 35].

I. Structure **a.** Normal (0) **b.** Surface Irregularity (1) **c.** Clefts to Transitional Zone (2) **d.** Clefts to Radial Zone (3) **e.** Clefts to Calcified Zone (4) **f.** Complete Disorganization (5)	**II. Cells** **a.** Normal (0) **b.** Diffuse Hypercellularity (1) **c.** Cloning (2)
III. Tidemark Integrity **a.** Normal/Intact (0) **b.** Duplicated Tidemark (1) **c.** Vascular Invasion Through one Tidemark (2) **d.** Vascular Invasion Through Second Tidemark (3)	**IV. Safranin-O Staining** **a.** Normal (0) **b.** Slight Reduction (1) **c.** Moderate Reduction (2) **d.** Severe Reduction (3)

Table 2

Averaged parameters of PLS cross-validation and prediction models* for modified Mankin score (MMS).

Average PLS Parameters (N = 3 models, ± Standard Deviation)	
RMSE	1.06 (±0.01)
RMSEP	1.41 (±0.15)
Percent correct PLS spectral predictions	72 (±3.1)%
Percent correct PLS spectral predictions within one grade of actual MMS	96 (±1.4)%

* Multiplicative scatter corrected (MSC) second derivative spectra and 7 factors were used in all models. Cross-validation models were created from ~2/3 of the total data set (100 spectra) of 152 spectra, and the remaining 52 spectra used for independent prediction. Root mean square error (RMSE) of validation was measured to determine the overall error of the cross-validation model. The root mean square error of prediction (RMSEP) was calculated from the independent prediction of 52 spectra.

Table 3

FT-IRIS measurements of full depth cartilage parameters.

MMS	N	Collagen	PG	Collagen Integrity	Collagen Maturity	Parallel	Random	Perpendicular
2	5	26.6±4.6	3.8±0.6	0.024±0.003	3.2±0.1	35.06±18.8	58.3±13.1	6.6±1.2
3	3	24.5±3.1	3.8±0.4	0.023±0.003	3.0±0.2	32.9±13.05	67.0±13.03	0.01±0.02*
4	3	30.8±1.7	5.4±0.2	0.016±0.013	3.0±0.05	36.4±18.9	62.6±17.5	0.8±1.4*
5	2	43.4±2.1	5.8±0.2	0.021±0.005	3.0±0.0	2.5±1.3*	77.5±19.4*	19.9±18.03*
6	3	24.8±2.1	4.2±0.6	0.018±0.005	2.9±0.1*	10.1±10.9*	88.9±11.06*	0.9±0.6*
7	3	48.7±3.4	8.0±0.6	0.023±0.002	2.9±0.1*	12.2±12.8*	75.2±2.6*	12.4±11.4
8	3	28.8±1.9	4.3±0.2	0.022±0.002	2.9±0.1*	8.5±1.6*	91.4±1.6*	0.002±0.00*
9	3	19.3±7.3	3.7±0.7	0.029±0.011	3.0±0.05	9.6±13.03*	72.3±2.1*	17.1±15.2
10	3	51.1±3.0	5.8±0.1	0.025±0.000	2.83±0.03*	7.0±4.1*	52.3±27.5	40.6±31.3*

MMS = Modified Mankin Score; N = sample size.

Values are mean ± standard deviation over the full sample thickness. The orientation values (parallel, random, perpendicular) indicate the percentage of pixels for each orientation over the full sample thickness.

*Significantly different from MMS 2 samples ($p < 0.05$).